



Short communication

Porous $\text{Co}_3\text{O}_4/\text{NiO}$ core/shell nanowire array with enhanced catalytic activity for methanol electro-oxidation

J.B. Wu*, Z.G. Li, X.H. Huang, Y. Lin

School of Physics & Electronic Engineering, Taizhou University, 1139 Shifu Avenue, Jiaojiang, Taizhou 318000, Zhejiang, China

H I G H L I G H T S

- Construct a self-supported porous $\text{Co}_3\text{O}_4/\text{NiO}$ core/shell nanowire array.
- Core/shell nanowire array shows high electro-oxidation property of methanol.
- Core/shell nanowire array structure is favourable for fast ion and electron transfer.

A R T I C L E I N F O

Article history:

Received 9 August 2012

Received in revised form

20 September 2012

Accepted 23 September 2012

Available online 28 September 2012

Keywords:

Nickel oxide

Cobalt oxide

Core/shell

Nanowire array

Methanol electro-oxidation

A B S T R A C T

A self-supported $\text{Co}_3\text{O}_4/\text{NiO}$ core/shell nanowire array is prepared by the combination of hydrothermal synthesis and electro-deposition methods. The $\text{Co}_3\text{O}_4/\text{NiO}$ core/shell nanowire array shows a combined structure of mesoporous nanowire core and branch nanoflakes shell as well as hierarchically porous structure. The electro-oxidation properties of methanol of the $\text{Co}_3\text{O}_4/\text{NiO}$ core/shell nanowire array are elucidated by cyclic voltammetry (CV) and chronoamperometry tests. Impressively, the $\text{Co}_3\text{O}_4/\text{NiO}$ core/shell nanowire array exhibits much higher electro-catalytic activity, lower over-potential and much more stability for methanol electro-oxidation compared to the single Co_3O_4 nanowire array in alkaline medium. The enhancement of the electro-catalytic reactivity is due to the synergistic effect and unique porous core/shell nanowire architecture, which provides fast ion/electron transfer, sufficient contact between active materials and electrolyte, leading to faster kinetics, lower over-potential and higher electro-catalytic reactivity.

© 2012 Elsevier B.V. All rights reserved.

1. Introduction

Direct methanol fuel cell (DMFC) is considered as a promising candidate for future energy demand due to its high energy conversion efficiency, low operating temperature and low pollutant emission [1]. Nevertheless, its practical application is hindered by high over-potential associated with the direct electro-oxidation of methanol. Although Pt [2], Ru [3], Pd [4], and their alloys catalysts [5,6], have been demonstrated with excellent electro-catalytic activities, the high cost and low utilization of these materials limit their commercial applications. Hence, considerable efforts have been made to search for alternative low-cost transition metal oxides/hydroxides (such as NiO, Co_3O_4 , CoO, $\text{Ni}(\text{OH})_2$ and $\text{Co}(\text{OH})_2$) catalysts for DMFC [7–10]. Particularly, NiO and Co_3O_4 are attractive catalysts for direct electro-oxidation of methanol due to their

lower cost and high electrocatalytic activity. It is well accepted that the performance of transition metal oxides catalysts is mainly governed by the electrochemical activity and kinetic feature of the active materials. In a nutshell, it is crucial to enhance the kinetics of ion and electron transport in electrodes and at the electrode/electrolyte interface to improve the electro-catalytic activity.

Currently, several strategies have been taken to construct high-performance transition metal oxides catalysts for DMFC. One way is direct growth of nanoarrays of metal oxides on current collectors. On one hand, this integrated electrode ensures good mechanical adhesion and electric connection of the active material to the current collector. On the other hand, the designed nanoarrays electrodes show highly porous structures embodied in the form of nanotubes, nanowires, nanorods or random nanoporous structures. These highly porous structures provide short transportation path for both electrons and ions, thus leading to fast reaction kinetics. Another fascinating strategy is to scrupulously construct smart hybridization of bespoke active materials, namely, to combine different active metal oxides into the single electrode to take the

* Corresponding author. Tel.: +86 576 88661937.

E-mail address: wujb@tzc.edu.cn (J.B. Wu).

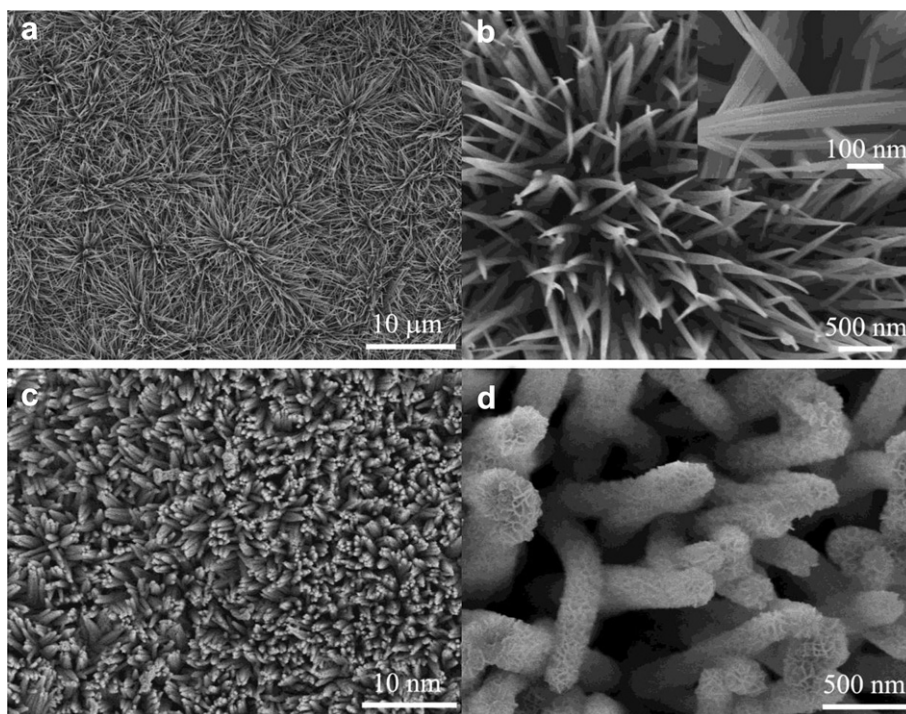


Fig. 1. SEM images of (a), (b) Co_3O_4 nanowire array (fine structure in inset) and (c), (d) $\text{Co}_3\text{O}_4/\text{NiO}$ core/shell nanowire array on nickel foam.

advantages of both components and offer special properties through the reinforcement or modification of each other [11], resulting in enhanced electro-catalytic performances. This has been proven as an effective way to combine the merits of the individual components. For example, nanostructured Pd–NiO/C [12], Pt–NiO/C [13], NiO/MgO [14], have been successfully fabricated and

improved results have been demonstrated for direct electro-oxidation of methanol.

Based on the above two issues, we find core/shell nanowire heterostructured arrays can meet the requirements for designing high-performance catalysts for direct electro-oxidation of methanol. First, their one-dimensional (1D) nanostructures can provide

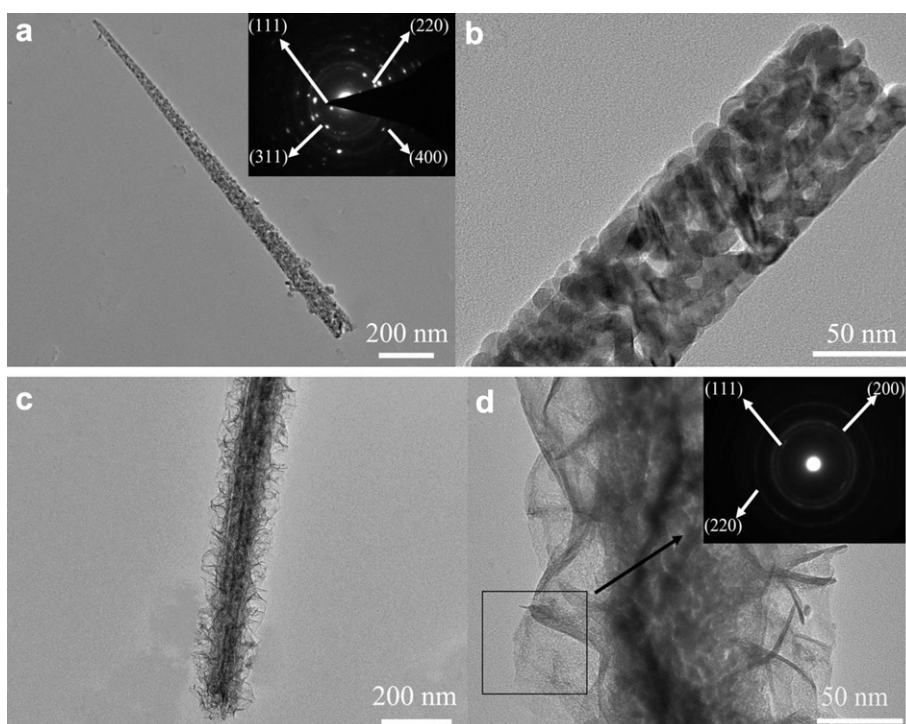


Fig. 2. TEM images of (a), (b) Co_3O_4 nanowire (SAED pattern in inset) and (c), (d) $\text{Co}_3\text{O}_4/\text{NiO}$ core/shell nanowire (SAED pattern in inset).

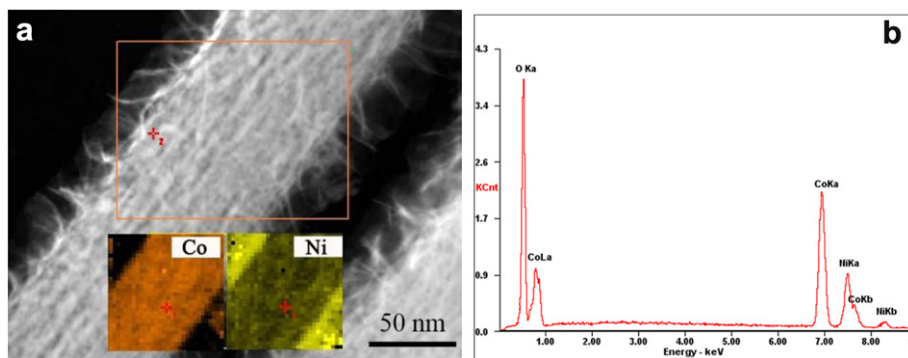


Fig. 3. (a) EDS maps of Co and Ni and (b) EDS spectrum of $\text{Co}_3\text{O}_4/\text{NiO}$ core/shell nanowire.

short diffusion path for ions and electrons to achieve fast redox reactions with high energy conversion efficiency and fast reaction kinetics. Second, the structural features and electro-activities of each component are fully manifested in this composite structure. The interface/chemical distributions are homogeneous at a nano-scale size. Third, the core/shell nanowire heterostructures integrate different active materials into a single electrode to take the advantages of both components and offer special properties through the reinforcement or modification of each other, resulting in enhanced electro-catalytic reactivity. In the present work, we report a self-supported $\text{Co}_3\text{O}_4/\text{NiO}$ core/shell nanowire array on nickel foam by the combination of hydrothermal synthesis and electro-deposition methods. The obtained core/shell nanowires have a combined structure of mesoporous nanowire core and branch nanoflakes shell as well as porous morphology. The $\text{Co}_3\text{O}_4/\text{NiO}$ core/shell nanowire array presents noticeable catalytic activity and electrochemical stability for the electro-oxidation of methanol.

2. Experimental

All solvents and chemicals were of reagent quality and used without further purification. The cobalt nitrate, nickel sulphate, sodium sulphate, sodium acetate, urea and ammonia fluoride were obtained from Shanghai Chemical Reagent Co. All aqueous solutions were freshly prepared with high purity water (18 M Ω cm resistance).

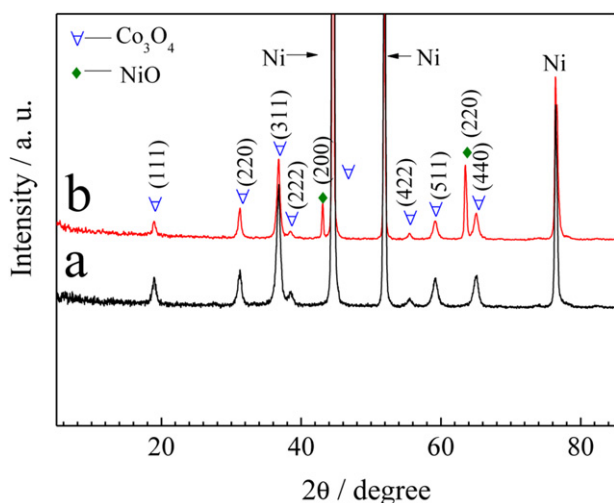


Fig. 4. XRD patterns of (a) Co_3O_4 nanowire array and (b) $\text{Co}_3\text{O}_4/\text{NiO}$ core/shell nanowire array on nickel foam.

The experimental details were as follows. The self-supported $\text{Co}_3\text{O}_4/\text{NiO}$ core/shell nanowire array was prepared as follows. Firstly, the Co_3O_4 nanowire array was prepared by a facile hydrothermal synthesis method described in detail in previous work [11]. In a typical synthesis, the reaction solution consisted of 2 mmol of $\text{Co}(\text{NO}_3)_2$, 4 mmol NH_4F , 10 mmol of $\text{CO}(\text{NH}_2)_2$ and 50 mL of distilled water. Clean nickel foam was used as the substrate and its top side was coated with a polytetrafluoroethylene tape to prevent contamination. The liner was sealed in a stainless steel autoclave and maintained at 105 °C for 5 h, and then cooled down to room temperature. The samples were rinsed with distilled water several times and annealed at 350 °C in normal purity argon for 2 h. Then, the self-supported Co_3O_4 nanowire array was used as the scaffold for NiO nanoflake shell growth via a simple electro-deposition method performed in a three-compartment system at 25 °C, the above Co_3O_4 nanowire array as the working electrode, saturated calomel electrode (SCE) as a reference electrode and a Pt foil as a counter-electrode. The electrolyte for electro-deposition was made up of 0.13 M nickel sulphate, 0.13 M Na_2SO_4 and 0.1 M sodium acetate, in which sodium acetate was the buffer solution to keep pH value between 6.5 and 7.5 during the entire deposition process [15]. The electro-deposition experiment was carried out at a constant anodic current of 0.25 mA cm $^{-2}$ for 1 h. Then, the samples were rinsed with distilled water and annealed at 300 °C in argon for 1.5 h to form $\text{Co}_3\text{O}_4/\text{NiO}$ core/shell nanowire array. The load weight of Co_3O_4 and NiO in the core/shell array was about 1.5 mg cm $^{-2}$ and 0.5 mg cm $^{-2}$.

The morphology and microstructure of samples were characterized by X-ray diffraction (XRD, RIGAKU D/Max-2550 with Cu K α radiation), field emission scanning electron microscopy (FESEM, FEI SIRION) and high-resolution transmission electron microscopy (HRTEM, JEOL JEM-2010F). The electrochemical measurements were carried out in a three-electrode electrochemical cell. 1 M KOH and 1 M KOH + 0.5 M methanol solutions were used as the electrolytes, respectively. Cyclic voltammetry (CV) measurements were performed a scanning rate of 25 mV s $^{-1}$ at 25 °C on a CHI660c electrochemical workstation (Chenhua, Shanghai) with the core/shell array as the working electrode, a Hg/HgO (0.098 V vs. SHE) as the reference electrode and a Pt foil as the counter-electrode. The chronoamperometry tests were conducted under the potential of 0.55 V (vs. SHE) for 1000 s.

3. Results and discussion

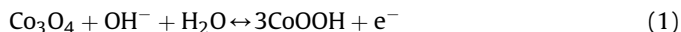
The self-supported $\text{Co}_3\text{O}_4/\text{NiO}$ core/shell nanowire array on nickel foam is successfully prepared via the combination of hydrothermal synthesis and electrochemical deposition methods. The first step of our approach involves the hydrothermal synthesis

of freestanding Co_3O_4 nanowire array. Then the Co_3O_4 nanowire array acts as the backbone for conformal electro-deposition of NiO branch nanoflakes shell to create core/shell nanowire array. The whole surface of the nickel foam is uniformly covered by the hydrothermal-synthesized Co_3O_4 nanowires with diameters of ~ 80 nm (Fig. 1a and b). After electro-deposition with heat treatment, the Co_3O_4 nanowires are intimately decorated by NiO branch nanoflakes with diameters of ~ 10 nm to form core/shell nanowire array (Fig. 1c and d). Moreover, the NiO branch nanoflakes are connected with each other to form net-like porous structure possessing pore diameters of 10–100 nm.

The detailed porous core/shell nanowire structure is further demonstrated by the TEM images. The individual Co_3O_4 nanowire shows mesoporous structure with pores ranging from 2 to 5 nm (Fig. 2a and b). The Co_3O_4 nanowire is made up of numerous interconnected nanoparticles with sizes of 2–10 nm. In addition, all diffraction rings in the selected area electronic diffraction (SAED) pattern of the nanowire can be well indexed with the spinel Co_3O_4 phase (JCPDS 42-1467), indicating that the Co_3O_4 nanowire is crystalline in nature. For the individual core/shell nanowire, it is clearly shown that the Co_3O_4 nanowire is tightly wrapped by the electrodeposited NiO nanoflakes shell (Fig. 2c and d). Besides, the SAED pattern of the nanoflakes shell reveals the existence of cubic polycrystalline NiO (JCPDS 4-0835), indicating the formation of $\text{Co}_3\text{O}_4/\text{NiO}$ core/shell nanowire array. X-ray spectroscopy (EDS) elemental mapping of Co and Ni (Fig. 3a) unambiguously confirms the $\text{Co}_3\text{O}_4/\text{NiO}$ core/shell hierarchical structure. The mapping result is consistent with the EDS spectrum shown in Fig. 3b. X-ray diffraction (XRD) pattern shows that the core/shell nanowire arrays

contain spinel Co_3O_4 phase (JCPDS 42-1467) and cubic NiO phase (JCPDS 4-0835) (Fig. 4). Taking the above results together, the as-prepared $\text{Co}_3\text{O}_4/\text{NiO}$ core/shell nanowire array exhibits highly porous array configuration which is favourable for fast ion/electron transport and enhanced electrochemical reactivity can be anticipated.

The electro-oxidation properties of methanol of the $\text{Co}_3\text{O}_4/\text{NiO}$ core/shell nanowire array are elucidated by cyclic voltammetry (CV) and chronoamperometry tests. Fig. 5a displays the CV curves of the $\text{Co}_3\text{O}_4/\text{NiO}$ core/shell nanowire array and single Co_3O_4 nanowire array measured at a scanning rate of 25 mV s^{-1} . For the single Co_3O_4 nanowire array, the redox couple A1/A2 is owing to the conversion between CoOOH and Co_3O_4 as follows [16].



For the $\text{Co}_3\text{O}_4/\text{NiO}$ core/shell nanowire array, only one redox couple P1/P2 is observed. This redox couple P1/P2 is an integrated redox couple probably due to the integration of redox couple of NiO/NiOOH and redox couple $\text{CoOOH}/\text{Co}_3\text{O}_4$ because these two redox couples have similar reaction potentials. Notice that the enclosed area of CV loop of the $\text{Co}_3\text{O}_4/\text{NiO}$ core/shell nanowire array is larger than the single Co_3O_4 nanowire array. Besides, the current densities of the $\text{Co}_3\text{O}_4/\text{NiO}$ core/shell nanowire array are higher than those of the single Co_3O_4 nanowire array, implying its better electrochemical reactivity.

The electro-oxidation of methanol of these two nanowire arrays is clearly observed by the CV in the 0.5 M methanol + 1 M KOH solution at a scanning rate of 25 mV s^{-1} (Fig. 5b). A sharp increase in

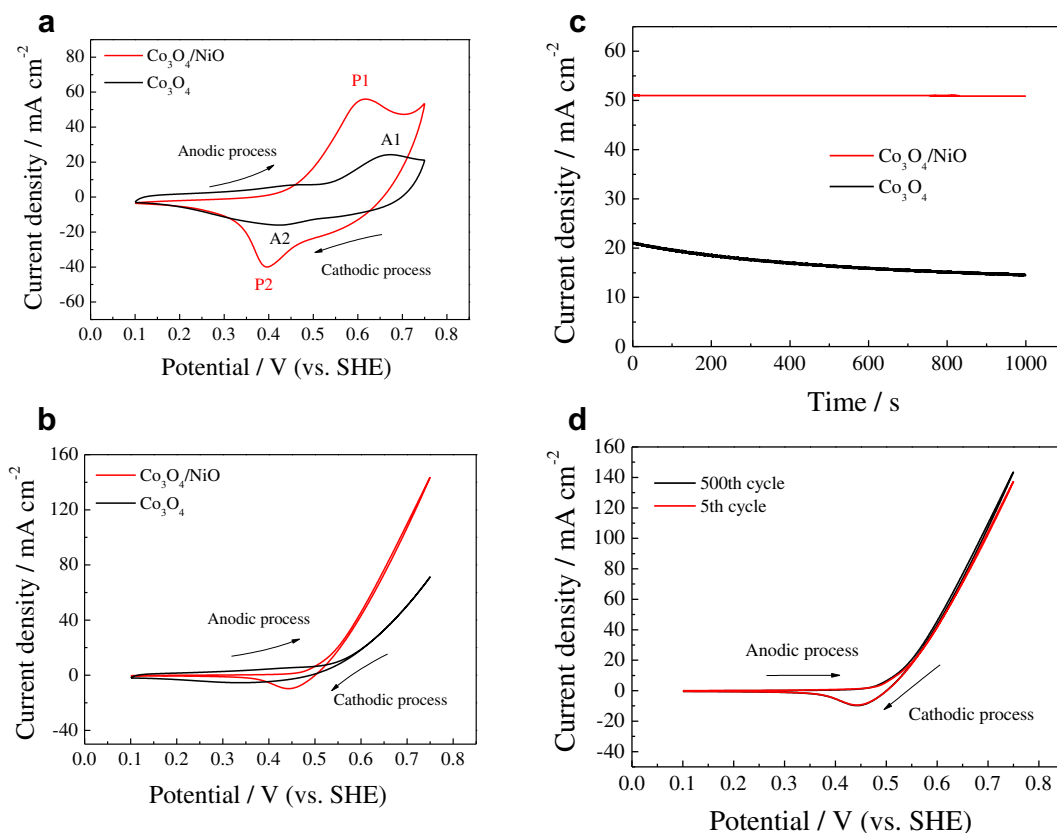
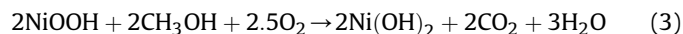
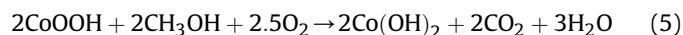
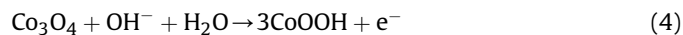


Fig. 5. Cyclic voltammograms of the Co_3O_4 nanowire array and $\text{Co}_3\text{O}_4/\text{NiO}$ core/shell nanowire array measured in different electrolytes (a) 1 M KOH and (b) 1 M KOH + 0.5 M methanol solutions at a scanning rate of 25 mV s^{-1} . (c) Chronoamperometric curves of the Co_3O_4 nanowire array and $\text{Co}_3\text{O}_4/\text{NiO}$ core/shell nanowire array in 1 M KOH + 0.5 M methanol solution at the potential of 0.55 V (vs. SHE) for 1000 s. (d) CV curves of $\text{Co}_3\text{O}_4/\text{NiO}$ core/shell nanowire array measured at different cycles in 1 M KOH + 0.5 M methanol solutions at a scanning rate of 25 mV s^{-1} .

the anodic current density for methanol oxidation is noticed. The mechanism of electro-oxidation of methanol on NiO and Co₃O₄ may be simply illustrated by the following reactions, respectively [7,10,17].



And



The Co₃O₄/NiO core/shell nanowire array shows high anodic current density with almost two times larger than that of the single Co₃O₄ nanowire array. Furthermore, the start potential of electro-oxidation of methanol for the Co₃O₄/NiO core/shell nanowire array is approximately at 0.45 V (vs. SHE), much lower than the single Co₃O₄ nanowire array (about 0.55 V vs. SHE), meaning that the core/shell nanowire array has much lower over-potential for direct electro-oxidation of methanol. Besides, the performance of electro-oxidation of methanol of the Co₃O₄/NiO core/shell nanowire array is much better than those of Co(OH)₂ [9], Ni(OH)₂ [8], NiO powders [18] and NiO/CNTs composites [19], and comparable to those of Pt–NiO/C composites [13,20]. Nevertheless, the onset electro-oxidation potential of methanol of the Co₃O₄/NiO core/shell nanowire array is still much higher than well-known Pt, Ru, Pd catalysts (onset potential is ~ -0.35 V vs. SHE) [21–25]. The high electro-oxidation potential is the main obstacle for the commercialization of metal oxides catalysts for DMFC. This phenomenon exists in all metal oxides/hydroxides catalysts for alkaline DMFC [8,9,18,19]. Even so, metal oxides catalysts are still attracting more and more attention due to its low cost and high electrocatalytic activity. Hence, there still much space for progress to achieve satisfactory electrocatalytic performance of metal oxides for practical application. The electrochemical stability is measured by chronoamperometry (Fig. 5c). The Co₃O₄/NiO core/shell nanowire array does not show any decay, but exhibits more stable and higher reaction current than the single Co₃O₄ nanowire array, indicating its improved electrochemical stability. We also compared CV curves of the Co₃O₄/NiO core/shell nanowire array at 5th and 500th cycles (Fig. 5d). Note that the CV curve is quite stable after 500 cycles and the anodic current density is even higher than the 5th cycle, demonstrating its excellent cycle stability. The enhanced electro-catalytic reactivity is mainly due to the unique porous core/shell architecture providing several major advantages: (1) Both Co₃O₄ and NiO are catalysts for direct electro-oxidation of methanol. They can work together and provide potential synergistic effect contributing to the higher electro-catalytic reactivity. (2) The directly grown array ensures good mechanical adhesion and electrical connection to the current collector and avoids the use of polymer binders and conducting additives. (3) The porous core/shell array architecture enables the fully exposure of both active materials to the electrolyte and provides short diffusion path for both electrons and ions, thus leading to faster kinetics, lower over-potential and higher electro-catalytic reactivity.

4. Conclusion

In summary, a self-supported Co₃O₄/NiO core/shell nanowire array is prepared by the combination of hydrothermal synthesis and electro-deposition methods. The Co₃O₄/NiO core/shell nanowire array possesses a hierarchical porous architecture consisting of mesoporous core and branch nanoflakes shell. Compared to the single Co₃O₄ nanowire array, the Co₃O₄/NiO core/shell nanowire array exhibits higher electrochemical catalytic ability, lower over-potential and more stability for methanol oxidation reaction. The improved electro-catalytic reactivity is attributed to the unique porous core/shell nanowire configuration. Our research provides a promising new class of catalyst for methanol oxidation or other advanced catalytic reaction.

Acknowledgement

The authors would like to acknowledge financial support from Zhejiang Provincial Natural Science Foundation of China (Grant No. Y4110628) and National Natural Science Foundation of China (Grant No. 51204116).

References

- [1] Y. Lu, J.P. Tu, C.D. Gu, X.H. Xia, X.L. Wang, S.X. Mao, J. Mater. Chem. 21 (2011) 4843.
- [2] Y.P. Bi, G.X. Lu, Electrochem. Commun. 11 (2009) 45.
- [3] S. Garbarino, A. Ponrouch, S. Pronovost, D. Guay, Electrochem. Commun. 11 (2009) 1449–1452.
- [4] D.S. Yuan, C.W. Xu, Y.L. Liu, S.Z. Tan, X. Wang, Z.D. Wei, P.K. Shen, Electrochem. Commun. 9 (2007) 2473.
- [5] T. Huang, J.L. Liu, R.S. Li, W.B. Cai, A.S. Yu, Electrochem. Commun. 11 (2009) 643.
- [6] H. Wang, C.W. Xu, F.L. Cheng, M. Zhang, S.Y. Wang, S.P. Jiang, Electrochem. Commun. 10 (2008) 1575.
- [7] M. Asgari, M.G. Maragheh, R. Davarkhah, E. Lohrasbi, J. Electrochem. Soc. 158 (2011) K225.
- [8] A.A. El-Shafei, J. Electroanal. Chem. 471 (1999) 89.
- [9] M. Jafarian, M.G. Mahjani, H. Heli, F. Gobal, H. Khajehsharifi, M.H. Hamed, Electrochim. Acta 48 (2003) 3423.
- [10] S. Zafeirotas, T. Dintzer, D. Teschner, R. Blume, M. Havecker, A. Knop-Gericke, R. Schlögl, J. Catal. 269 (2010) 309.
- [11] X. Xia, J. Tu, Y. Zhang, X. Wang, C. Gu, X.-b. Zhao, H.J. Fan, ACS Nano 6 (2012) 5531.
- [12] M.L. Wang, W.W. Liu, C.D. Huang, Int. J. Hydrogen Energy 34 (2009) 2758.
- [13] R.S. Amin, R.M.A. Hameed, K.M. El-Khatib, M.E. Youssef, A.A. Elzatahy, Electrochim. Acta 59 (2012) 499.
- [14] C. Mahendiran, T. Maiyalagan, K. Scott, A. Gedanken, Mater. Chem. Phys. 128 (2011) 341.
- [15] M.S. Wu, C.H. Yang, Appl. Phys. Lett. 91 (2007) 033109.
- [16] J.P. Liu, J. Jiang, C.W. Cheng, H.X. Li, J.X. Zhang, H. Gong, H.J. Fan, Adv. Mater. 23 (2011) 2076.
- [17] H. Heli, H. Yadegari, Electrochim. Acta 55 (2010) 2139.
- [18] N. Spinner, W.E. Mustain, Electrochim. Acta 56 (2011) 5656.
- [19] X. Tong, Y. Qin, X. Guo, O. Moutanabbir, X. Ao, E. Pippel, L. Zhang, M. Knez, Small (2012). <http://dx.doi.org/10.1002/smll.201200839>.
- [20] D.B. Kim, H.J. Chun, Y.K. Lee, H.H. Kwon, H.I. Lee, Int. J. Hydrogen Energy 35 (2010) 313.
- [21] Z.W. Liu, Q.Q. Shi, F. Peng, H.J. Wang, H. Yu, J.C. Li, X.Y. Wei, Catal. Commun. 22 (2012) 34.
- [22] J.H. Jiang, T. Aulich, J. Power Sources 209 (2012) 189.
- [23] S.S. Mahapatra, A. Dutta, J. Datta, Int. J. Hydrogen Energy 36 (2011) 14873.
- [24] D.H. Duan, Z.L. Zhang, T. Zhang, S.B. Liu, X.G. Hao, Y.B. Li, Chem. J. Chin. Univ. 32 (2011) 2618.
- [25] H.P. Liu, J.Q. Ye, C.W. Xu, S.P. Jiang, Y.X. Tong, J. Power Sources 177 (2008) 67.